# Adsorbate-Promoted Tunneling-Electron-Induced Local Faceting of D/Pd{110}-(1 × 2)

**ARTICLE** *in* JOURNAL OF PHYSICAL CHEMISTRY LETTERS · JULY 2010

Impact Factor: 7.46 · DOI: 10.1021/jz100640y



**5 AUTHORS**, INCLUDING:

Patrick Han
Tohoku University
**25** PUBLICATIONS **593** CITATIONS
SEE PROFILE

Andrea N Giordano Bills
St. John Fisher College
**13** PUBLICATIONS **70** CITATIONS
SEE PROFILE

Paul S Weiss
University of California, Los Angeles
**395** PUBLICATIONS **11,932** CITATIONS
SEE PROFILE

THE JOURNAL OF PHYSICAL CHEMISTRY Letters

pubs.acs.org/JPCL

# Adsorbate-Promoted Tunneling-Electron-Induced Local Faceting of D/Pd{110}-(1 × 2)

Adam R. Kurland,[†] Patrick Han,[†] John C. Thomas,[†] Andrea N. Giordano,[†] and Paul S. Weiss*[,†,‡]

[†]Departments of Chemistry and Physics, The Pennsylvania State University, University Park, Pennsylvania 16802, and [‡]California NanoSystems Institute and Departments of Chemistry and Biochemistry, University of California, Los Angeles, Los Angeles, California 90095

**ABSTRACT** We have utilized tunneling electrons and thiophene adsorption to draw deuterium (D) from within the single-crystal bulk beneath Pd{110} up to subsurface adsorption sites. We found local faceting induced by this process, and determined the energy threshold of drawing bulk D to subsurface sites to be 0.38 ± 0.02 eV. We show that these facets propagate along the ⟨1$\bar{1}$0⟩ direction of the substrate, and that Pd{110} adopts the (1 × 1) surface reconstruction on the induced facets, yet maintains the paired row (1 × 2) structure on unaffected regions. After producing subsurface D, the facet plane tilts 3.2 ± 0.8° off the substrate plane.

SECTION Surfaces, Interfaces, Catalysis

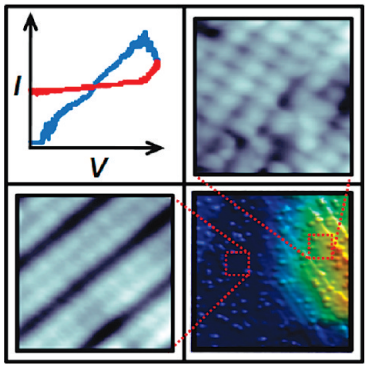


Molecular-scale heterogeneous catalysis studies elucidate reaction mechanisms critical to technological processes, with the ultimate goal of improving catalyst design from the bottom up.[1] Major advances have resulted from the fabrication of metallic and bimetallic supported catalysts for a wide variety of catalytic reactions using shape-controllable synthetic approaches,[2,3] and "self-activating" catalytic systems involving surface and subsurface hydrogen (H) or deuterium (D) in the selective partial hydrogenation of small alkenes.[4] Transition and near-noble metals, specifically palladium (Pd), play important roles in catalyst design and function because of their behavior when modified by H or D adsorption and absorption.[5−7] It is understood that both the physical and electronic landscape of the metal substrate influence the coincidence and interactions of adsorbed molecules through substrate-mediated interactions (SMIs), even at catalytically relevant temperatures.[8−12] However, catalyst design is hindered by the complexity and incomplete understanding of the mechanisms of the catalytic reactions. For instance, hydrogenation on Pd is known to depend strongly on both the surface structure *and* on the distribution of heteroatom species on *and* beneath the metal surface.[13−19] The dissolution of hydrogen into metal subsurface sites and its effects on surface adsorbates has been addressed in a review by Christmann and references therein highlighting ensemble spectroscopic techniques such as low-energy electron diffraction (LEED), Auger electron spectroscopy (AES), temperature-programmed desorption (TPD), and high-resolution electron energy loss spectroscopy (HREELS).[20] Additionally, the subsurface hydride of Pd{111} has been revealed directly by scanning tunneling microscopy (STM).[16−18,21,22] A recent advance by Teschner et al. demonstrated that this subsurface species, along with subsurface carbon impurities, impact catalytic selectivity through localized surface structural transitions.[19]

In this work, we use the direct, local probe of our ultrastable, extreme high vacuum (XHV) cryogenic (4 K) STM[23] to elucidate these surface transitions on the atomic scale and with direct local spectroscopic characterization. We study the D/Pd{110} catalytic system beginning with D-induced surface reconstruction and discover local faceting of the D/Pd{110}-(1 × 2) surface upon thiophene adsorption followed by application of tunneling electrons. Initial reconstruction of Pd{110} by D adsorption follows the (1 × 2) row pairing mechanism.[24] Subsequent adsorption of thiophene combined with the perturbation by the STM tip drives the formation of localized (1 × 1) facets tilting off the plane of the underlying substrate to facilitate the population of subsurface sites by D.

Induced facet reconstruction is known to occur on a variety of surfaces, both by molecular chemisorption[25−29] and by epitaxial growth during metal deposition.[30−32] Analyses by Madey and co-workers have followed surface reconstruction and faceting induced by epitaxial growth of ultrathin metallic films of Pd on tungsten and molybdenum surfaces.[33−36] However, whether induced by molecular adsorption or by epitaxial growth, faceting in these instances occurs in a fashion parallel to the plane of the underlying substrate lattice. Out-of-plane faceting has been observed for vicinal Cu{100} in the presence of oxygen.[37] There are few examples of achieving local control via STM,[38,39] and none address the impact of subsurface species on adsorbate-induced faceting. Thus, this work provides new insight into how adsorbates influence local structure of catalyst surfaces in the presence of surface and/or subsurface D, and how the

**Received Date:** May 16, 2010
**Accepted Date:** July 6, 2010
**Published on Web Date:** July 09, 2010





DOI: 10.1021/jz100640y | *J. Phys. Chem. Lett.* **2010**, *1*, 2288–2294

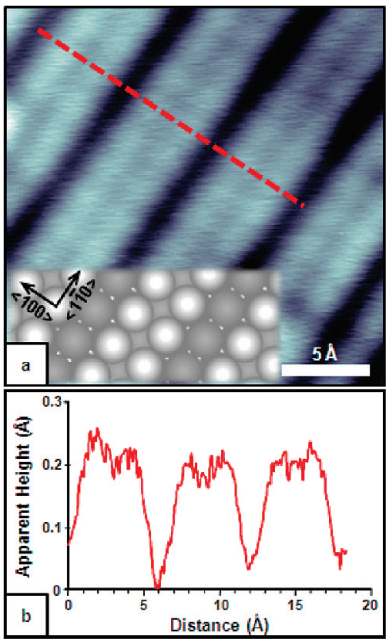


**Figure 1.** D-induced Pd{110}-(1 × 2) surface reconstruction. (a) Atomically resolved STM image (substrate bias voltage $V_s$ = 0.01 V; tunneling current $I_t$ = 1.4 nA; 22 Å × 22 Å) with model structure (inset) of the (1 × 2) phase. (b) Apparent height profile acquired along the dashed red line in panel a.

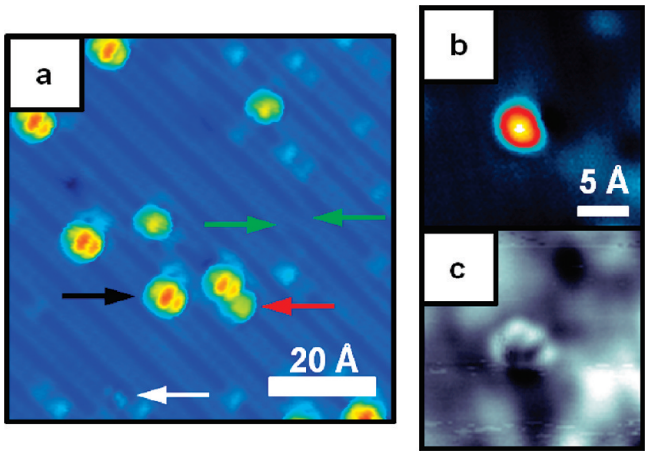


**Figure 2.** Thiophene adsorption on D/Pd{110}-(1 × 2) and on clean Pd{110}-(1 × 1). (a) Topographic STM image ($V_s$ = −0.015 V; $I_t$ = 0.2 nA; 73 Å × 73 Å) of thiophene deposited at low coverage on the D-reconstructed Pd{110}-(1 × 2) surface. Thiophene molecules appear as protrusions and adopt two distinct shapes/intensities in STM images depending upon adsorption site. (b) Topographic STM image ($V_s$ = 0.1 V; $I_t$ = 0.9 nA; 22 Å × 22 Å) of thiophene on Pd{110}-(1 × 1), accompanied by a simultaneously recorded differential conductance image, (c) showing enhancement of the local density of states (LDOS) at this energy. At positive sample bias, we observe lobes attributed to empty states.

individual components of heterogeneous catalytic systems work cooperatively, ultimately to affect chemical reactions.

Previous studies of H (D) on Pd{110} have focused on understanding the array of induced in-plane substrate reconstructions upon chemisorption.[40−49] Because Pd{110} is known to undergo surface reconstructions with and without H or D adsorption,[49−51] it is not surprising that additional chemisorption or coadsorption of other molecules can drive surface atoms toward energetically more favorable arrangements. Further, uptake of H or D into subsurface sites causes 6% outward relaxation relative to the bulk Pd lattice constant.[48] This was observed via differential conductance (d*I*/d*V*) STM imaging of surbsurface H in Pd{111}.[18] In addition, a recent study by Kralj et al. followed, directly, the initial stages of H-induced reconstruction of Pd{110} in situ by STM at room temperature.[52]

Here, we have chosen to study thiophene on D/Pd{110}-(1 × 2) because it provides insight into mechanisms of catalyst reactivity or poisoning, for instance in petroleum feedstocks, and because it has been used as a model toward elucidating the competing mechanisms of hydrogenation and hydrodesulfurization.[53−56] We study this system at 4 K to observe surface transitions and intermediate states that might not be accessible even fleetingly or observable at higher temperatures.

Adding D to a clean Pd{110} substrate results in the typical (1 × 2) surface reconstruction (Figure 1a). Figure 1b shows the height profile taken along the dashed red line in panel a, highlighting the row-pairing of this surface reconstruction. We use this and other similar images to confirm the reconstruction, and to show that contamination by subsurface impurities is minimal with our preparation procedure, limited to small amounts of atomic sulfur (S) contamination, as observed in our earlier work on Ni{110}[23] and in our previous investigations on Pd{111}.[14,18] We observe a small degree of S contamination even prior to thiophene deposition. The difficulty in removing S impurities stems from its concentration in the bulk of the crystal and its tendency to migrate to the surface and subsurface regions during annealing. The high-resolution STM image shown in Figure 1 was acquired such that no S was observed in the region.

Once the (1 × 2) surface was confirmed, we deposited thiophene to address local structural and electronic perturbations. The STM image in Figure 2a shows surface morphology after 4 K deposition of thiophene. We observe thiophene adsorption atop the paired rows (black arrow, Figure 2a), with some molecules of lower apparent height within the troughs between paired rows (red arrow, Figure 2a). The (1×2) surface also exhibits "railroad switch" structural perturbations (green arrows in Figure 2a) that are a result of the reconstruction. The d*I*/d*V* image acquired over a single thiophene molecule on the (1 × 1) surface (Figure 2c) reveals electronic lobes, yielding strong evidence that this molecule is lying flat on the surface. Hence, molecules lying atop the paired rows see more (1 × 1) structure locally and adopt the flat configuration, whereas the molecules adsorbed between paired rows bond through the sulfur and thus adopt a tilted conformation. Similarly, two distinct bonding orientations were also observed in our previous study of thiophene on Ni{110}.[57] Surface-bound S impurities are also apparent, denoted by the white arrow. The adsorption distribution as a result of possible SMIs will be discussed elsewhere, but may be attributed to the competition between the surface physical structure (i.e., the (1 × 1) versus the (1 × 2) paired row reconstructions) and the surface electronic structure of the Pd substrate.



DOI: 10.1021/jz100640y | J. Phys. Chem. Lett. 2010, 1, 2288–2294

In order to observe both the molecular structure of the thiophene adsorbates and the atomic structure of the underlying Pd surface, we typically scan at relatively high tunneling currents (> 1 nA) and low sample biases (< 100 mV). On the clean (1× 1) surface, we achieve the deconvolution of the molecular electronic structure (Figure 2c) acquired simultaneously with Figure 2b by d$I$/d$V$ imaging. Because we image in constant-current mode and at positive sample bias, we observe empty electronic states. The observed lobes account for the $\pi^*$ orbitals and are indicative of those observed in the STM simulations of thiophene on Pd{111}.[58]

On the (1 × 2) reconstruction, at larger $V_s$, molecular detail is lost, but higher conductance features increasingly appear in the area over which the STM probe rests between images. In Figure 3, topographic STM images show the result of hovering the tip over a thiophene-covered (white protrusions) D-reconstructed Pd surface. The phenomenon observed here after hovering over the center of the scan frame for 2 min at 1 V is manifested in the diffuse, higher-contrast feature in the center of the frame on the right (dotted circle in the right image of Figure 3). Subsequent hovering and scanning produces more prominent perturbations. Since other subsurface impurities

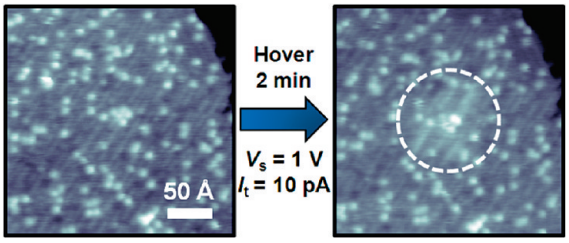


**Figure 3.** Drawing D to the subsurface sites of Pd{110}. The STM topographic image ($V_s$ = 0.5 V; $I_t$ = 0.010 nA; 260 Å × 260 Å) on the left was acquired before setting the bias voltage to 1 V. After setting the bias voltage to 1 V and having the STM tip hover in its rest position over the center of the frame for 2 min, the image on the right was acquired. A diffuse protruding region (dashed white circle) was observed at the center of the image.

are minimized by careful preparation, we attribute this effect to the population of subsurface sites by D atoms drawn up from the bulk Pd. Previously, we produced and imaged the subsurface hydride of Pd{111} at 4 K. We have shown that we can use ballistic scattering of tunneling electrons to draw and to manipulate bulk hydrogen to the stable subsurface region.[18] Whereas subsurface H in Pd{111} causes outward relaxation of the surface lattice on the order of a few hundredths of an Ångstrom, here, we observe a much different effect—one that occurs along the direction of the paired rows (the $\langle 1\bar{1}0\rangle$ direction) only in the presence of additional thiophene. In the absence of preadsorbed D, deposition of thiophene and subsequent imaging resulted in no apparent local structural perturbation (see Supporting Information, Figure S1a). Similarly, imaging the D-reconstructed surface shown in Figure 1 at larger $V_s$ (3 eV) in the absence of thiophene also produced no faceting (see Supporting Information, Figure S1b). It should be noted that the image in Figure S1b was acquired after obtaining 40 individual conductance spectra along the trajectory indicated by the red arrow from +1 to +4 eV with a total acquisition time of over 4 h. This energy range is well above the faceting threshold. Thus, we posit that adsorption of thiophene onto the D-reconstructed surface lowers the overall barrier to near-surface D diffusion, and may be coverage dependent, as indicated by the work in ref 4.

Significant restructuring of the surface occurs with repeated imaging, and is both energetically and kinetically driven. That is, we observe faster growth at higher $V_s$; restructuring also occurs at lower $V_s$ over longer times, but not below a threshold bias voltage (*vide infra*). New faceted steps propagate along the $\langle 1\bar{1}0\rangle$ direction with angularity incommensurate with the plane of the underlying substrate. Step edges are typically more catalytically active than terrace sites due to the charge dipole across the step and higher available coordination.[59−72] Here, the formation of new steps may be driven by the favorability of thiophene to be in proximity to these active sites in the presence of subsurface D. Figure 4 shows one such example of this surface restructuring,

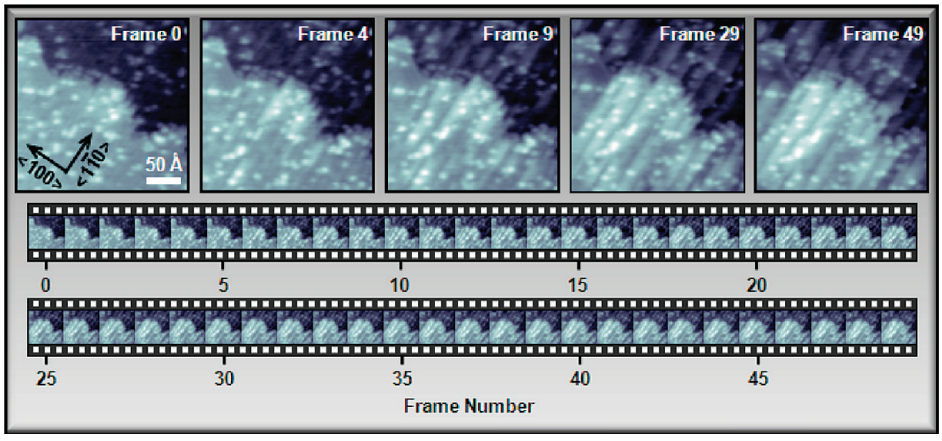


**Figure 4.** Selected frames extracted from a series of sequential STM images ($V_s$ = 1.0 V; $I_t$ = 0.05 nA; 260 Å × 260 Å) that were rendered into a time-lapse video file (Supporting Information). Already evident at the beginning of the sequence (Frame 0) is a more protruding region at the center of the image, where the STM probe rests for a short time (< 10 ms) before and between frame acquisition. Subsurface sites are increasingly populated as the tip rasters across the surface at $V_s$ = 1 V, and facets emerge and propagate along the $\langle 1\bar{1}0\rangle$ direction of the Pd{110} substrate. Population of the subsurface sites by D was saturated by frame 30.



DOI: 10.1021/jz100640y | J. Phys. Chem. Lett. 2010, 1, 2288–2294

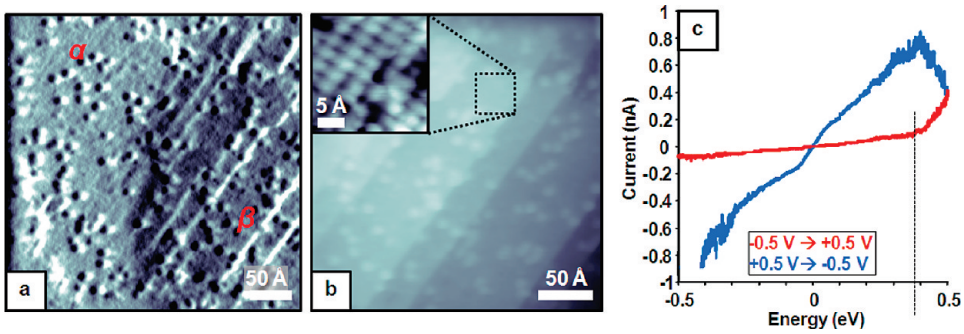


**Figure 5.** Determining the onset of the population of subsurface D in the presence of thiophene. (a) STM topographic (derivative) image ($V_s$ = 0.05 V; $I_t$ = 0.05 nA; 348 Å × 348 Å) highlighting the deviation of the facet planes ($\beta$) from the underlying substrate plane ($\alpha$). (b) Topographic STM image ($V_s$ = 0.05 V; $I_t$ = 0.05 nA; 260 Å × 260 Å) of region $\beta$ in panel a, plane subtracted (flattened by tilting the image). The inset is a high-resolution STM topographic image ($V_s$ = 0.01 V; $I_t$ = 1.4 nA; 22 Å × 22 Å) acquired over the region denoted by the black dotted box. Here, the Pd{110}-(1 × 1) structure has returned. The protrusions in both panels a and b are thiophene molecules. (c) Representative $I(V)$ spectrum taken over Pd in area α of panel a ($V_{gap}$ = 0.05 V; $I_{gap}$ = 0.05 nA). The red curve represents the forward bias sweep direction from negative to positive bias, and the blue curve represents the reverse sweep. Further spectra acquired at the same spot retraced the blue curve (see Figure S2 in the Supporting Information). The dashed line marks the onset value (0.38 ± 0.02 V) acquired from an average of 45 forward spectra at fresh locations on the surface.

highlighting individual images from 50 consecutive images acquired at 1 V. Faceting is nearly complete by frame 29, and little molecular diffusion is observed during faceting. Several time-lapse sequences acquired over up to 7 h and at a variety of sample bias voltages demonstrate that faceting is reliably induced at $|V_s| > 500$ mV.

To demonstrate that faceting is localized to the region imaged by the STM tip, we first created the facets at 1 V and then repositioned the tip to image both flat and faceted areas at small $V_s$. Scanning at lower $V_s$ prevents further subsurface D population. Figure 5a shows an area comprising both the (1 × 2) paired row surface (denoted α) and the faceted surface induced by scanning at 1 V (denoted $\beta$). These areas are shown prior to investigation by local $I(V)$ tunneling spectroscopy. Figure 5a is displayed in derivative mode to highlight the angularity of the stepped facets with respect to the flat underlying substrate. Using trigonometry, height profiles acquired and averaged over topographic images in this area (one such profile acquired over the dotted red line in Figure 5a) reveal that the faceted plane is tilted 3.2 ± 0.8° off the substrate plane. This small value is greatly exaggerated by the display used, as observed in Figure 5a, and accounts for the (1 × 1) structure over the $\beta$ region.

Figure 5b is an image acquired over the $\beta$ region, plane subtracted (flattened by tilting the image) to demonstrate that the angles of the faceted planes are identical within experimental error. The inset of Figure 5b shows a high-resolution scan resolving the Pd atoms in the (1 × 1) configuration over a faceted step, further confirmed by a fast Fourier transform (FFT) of the inset of Figure 5b (see Figure S3 in the Supporting Information).

Scanning tunneling spectroscopy (STS) over the paired row Pd{110} enables us to determine the onset voltage for D migration to the subsurface layer. The spectra in Figure 5c represent typical $I(V)$ curves for the faceting behavior (forward sweep in red and reverse sweep in blue) acquired over the α region. Bulk D is drawn to the subsurface region on the initial forward sweep, causing outward relaxation of the Pd lattice, thus, physically decreasing the probe-sample separation. Because of the exponential dependence between current and probe-sample separation, and because the STM probe is held at a fixed position during spectrum acquisition, this surface relaxation is observed as a steep onset in current response (dashed vertical line in Figure 5c). Since only a finite amount of bulk D can be drawn up into the subsurface region beneath the probe, we are able to acquire only one such spectrum in each location. Each spectrum displays the indicative onset in the forward sweep direction and the reconstructed surface signature on the reverse sweep. From 45 such spectra, we have determined the onset of drawing subsurface D to be 0.38 ± 0.02 eV. This $I(V)$ behavior is not observed over the (1 × 1) faceted regions of $\beta$, suggesting complete population of the subsurface sites with D. Subsequently recorded spectra have overlapping forward and reverse sweeps, as shown in Figure S2 in the Supporting Information. We point out a plausible correlation here with the STM images observed by Katano et al. (specifically that of Figure 8c of ref 4.). Their annealing at 202 K after additional molecular adsorption onto hydrogen precovered Pd{110} resulted in a vicinal surface. Here, we believe that we are observing the beginnings of this surface transformation by injecting tunneling electrons of sufficient energy relative to the thermal energy of annealing.

In this work, we have shown the propensity of the D/Pd{110}-(1 × 2) to undergo faceting along the $\langle 1\bar{1}0 \rangle$ direction after depositing thiophene and during observation by STM resulting from subsurface site population by D. At 4 K, this process requires additional local molecular adsorption in order to reduce the total surface free energy that might otherwise be achieved thermally, as in ref 4. Spectroscopic analysis reveals the onset of drawing subsurface D to be 0.38 ± 0.02 eV. Regions that do not show appreciable subsurface D exhibit the expected (1 × 2) surface reconstruction upon D adsorption, whereas faceted areas adopt the (1 × 1) atomic Pd configuration 3.2 ± 0.8° tilted with respect to the substrate plane. These differences in local surface structure account for the preferred adsorption sites found for thiophene between rows. Differential conductance imaging has elucidated the electronic LDOS of thiophene adsorbates, and may provide further insight into the bonding mechanism of this



DOI: 10.1021/jz100640y | J. Phys. Chem. Lett. 2010, 1, 2288–2294

and analogous heterocycles onto transition metal surfaces during hydrogenation, desulfurization, and deoxygenation.

We continue our studies of this system in order to develop a more comprehensive understanding of the catalytic reactions of small molecules on transition metals at the single-molecule scale, extending our spectroscopic capabilities to enhanced single-molecule vibrational measurements, theoretically modeled approaches, and subsequent action spectra.[10,14,73] This phenomenon has implications in elucidating key aspects of heterogeneous catalytic processes, including substrate structure changes,[74,75] directed modification of surface potential energy landscapes, and bulk diffusion. Additionally, these studies may provide insight into the mechanism responsible for metal embrittlement, and for developing routes toward stable, efficient, and clean hydrogen-storage materials.

## EXPERIMENTAL DETAILS

All experiments were carried out in a custom-built XHV (base pressure < $10^{-12}$ Torr), ultrastable, low temperature STM system with the additional capability of sample rotation for direct deposition of gas-phase molecules from the room temperature chamber onto the sample held at 4 K.[23] Tungsten probes were mechanically cut and sharpened in situ by high-voltage pulses.[76] The Pd{110} single crystal (MaTecK, GmbH) was prepared by cycles of $Ar^+$ sputtering at 875 K, oxygen treatment (~2 × $10^{-6}$ Torr at 875 K), and flash annealing to 1175 K. Sample cleanliness was ascertained by STM imaging prior to D or thiophene deposition. Molecular deuterium (Matheson Tri Gas, Parsippany, NJ) was deposited directly from a room temperature chamber onto the sample held at 4 K using a high-precision sapphire leak valve. Neat thiophene (Supelco, Bellefonte, PA) was further purified by several freeze−pump−thaw cycles and deposited directly from an identical high-precision sapphire leak valve. Purity and deposition of both deuterium and thiophene were monitored via a quadrupole residual gas analyzer (QMA 125, Balzers, Liechtenstein). The standard deposition parameters (deuterium, 180 Langmuir; thiophene, 480 Langmuir) were calibrated using an inverted magnetron cold cathode ion gauge at the main chamber, although the actual deposition incident on the sample can be up to 5 orders of magnitude lower due to the efficiency of cryopumping.[23] Ion pumps and gauges were turned off during actual deposition to avoid molecular fragmentation, and partial pressure was maintained by differentially pumping via a turbomolecular pump. Differential conductance imaging was performed by superimposing a small AC modulation ($\nu_{AC}$ = 1 kHz, $V_{rms}$ = 25 mV) on the DC sample bias, and then by monitoring the demodulated signal using a lock-in amplifier (SR850, Stanford Research Systems, Sunnyvale, CA). Topography and differential conductance images were acquired simultaneously. All bias voltages reported are sample biases ($V_s$) unless stated otherwise.

**SUPPORTING INFORMATION AVAILABLE** STM images of thiophene on Pd{110} in the absence of D and of the D-reconstructed surface in the absence of thiophene (Figure S1a,b, respectively), conductance spectra acquired over a (1×1) faceted area (Figure S2), the FFT of the STM image acquired over this area (Figure S3), and the video file showing increasing population of subsurface sites by D in Figure 4. This material is available free of charge via the Internet at http://pubs.acs.org.

## AUTHOR INFORMATION

### Corresponding Author:

*To whom correspondence should be addressed. E-mail: psw@cnsi.ucla.edu.

**ACKNOWLEDGMENT** The authors thank the Department of Energy (Grant #DE-FG02-08ER46546), the Petroleum Research Fund, and the Kavli Foundation for their generous support of this work.

## REFERENCES

(1) Bell, A. T. The Impact of Nanoscience on Heterogeneous Catalysis. *Science* **2003,** *299*, 1688–1691.
(2) Ahmadi, T. S.; Wang, Z. L.; Green, T. C.; Henglein, A.; El-Sayed, M. A. Shape-Controlled Synthesis of Colloidal Platinum Nanoparticles. *Science* **1996,** *272*, 1924–1926.
(3) Liu, C. K.; Zhou, Z. H.; Wu, Z. H.; Fransson, M.; Zhou, B. Shape-Controlled Synthesis and Catalytic Behavior of Supported Platinum Nanoparticles. *Synlett* **2009,** 595–598.
(4) Katano, S.; Kato, H. S.; Kawai, M.; Domen, K. Self-Activated Catalyst Layer for Partial Hydrogenation of 1,3-Butadiene on a Hydrogen-Precovered Pd(110) Surface. *J. Phys. Chem. C* **2009,** *113*, 14872–14878.
(5) Christmann, K. Interaction of Hydrogen with Solid-Surfaces. *Surf. Sci. Rep.* **1988,** *9*, 1–163.
(6) Ertl, G.; Knözinger, H.; Weitkamp, J. *Handbook of Heterogeneous Catalysis*; Wiley-VCH: Weinheim, Germany, 1997.
(7) Somorjai, G. A. *Introduction to Surface Chemistry and Catalysis*; John Wiley & Sons, Ltd.: New York, 1994.
(8) Han, P.; Kurland, A. R.; Thomas, J. C.; Giordano, A. N.; Weiss, P. S. To be submitted for publication.
(9) Mantooth, B. A.; Sykes, E. C. H.; Han, P.; Moore, A. M.; Donhauser, Z. J.; Crespi, V. H.; Weiss, P. S. Analyzing the Motion of Benzene on Au{111}: Single Molecule Statistics from Scanning Probe Images. *J. Phys. Chem. C* **2007,** *111*, 6167–6182.
(10) Nanayakkara, S. U.; Sykes, E. C. H.; Fernández-Torres, L. C.; Blake, M. M.; Weiss, P. S. Long-Range Electronic Interactions at a High Temperature: Bromine Adatom Islands on Cu{111}. *Phys. Rev. Lett.* **2007,** *98*, 206108.
(11) Sykes, E. C. H.; Han, P.; Kandel, S. A.; Kelly, K. F.; McCarty, G. S.; Weiss, P. S. Substrate-Mediated Interactions and Intermolecular Forces between Molecules Adsorbed on Surfaces. *Acc. Chem. Res.* **2003,** *36*, 945–953.
(12) Sykes, E. C. H.; Mantooth, B. A.; Han, P.; Donhauser, Z. J.; Weiss, P. S. Substrate-Mediated Intermolecular Interactions: A Quantitative Single Molecule Analysis. *J. Am. Chem. Soc.* **2005,** *127*, 7255–7260.
(13) Demchenko, D. O.; Sacha, G. M.; Salmeron, M.; Wang, L. W. Interactions of Oxygen and Hydrogen on Pd(111) Surface. *Surf. Sci.* **2008,** *602*, 2552–2557.
(14) Fernández-Torres, L. C.; Sykes, E. C. H.; Nanayakkara, S. U.; Weiss, P. S. Dynamics and Spectroscopy of Hydrogen Atoms on Pd{111}. *J. Phys. Chem. B* **2006,** *110*, 7380–7384.
(15) Ketteler, G.; Ogletree, D. F.; Bluhm, H.; Liu, H. J.; Hebenstreit, E. L. D.; Salmeron, M. In Situ Spectroscopic Study of the Oxidation and Reduction of Pd(111). *J. Am. Chem. Soc.* **2005,** *127*, 18269–18273.

(16) Mitsui, T.; Rose, M. K.; Fomin, E.; Ogletree, D. F.; Salmeron, M. Coadsorption and Interactions of O and H on Pd(111). *Surf. Sci.* **2002,** *511*, 259–266.

(17) Rose, M. K.; Borg, A.; Mitsui, T.; Ogletree, D. F.; Salmeron, M. Subsurface Impurities in Pd(111) Studied by Scanning Tunneling Microscopy. *J. Chem. Phys.* **2001,** *115*, 10927–10934.

(18) Sykes, E. C. H.; Fernández-Torres, L. C.; Nanayakkara, S. U.; Mantooth, B. A.; Nevin, R. M.; Weiss, P. S. Observation and Manipulation of Subsurface Hydride in Pd{111} and Its Effect on Surface Chemical, Physical, and Electronic Properties. *Proc. Natl. Acad. Sci. U.S.A* **2005,** *102*, 17907–17911.

(19) Teschner, D.; Borsodi, J.; Wootsch, A.; Revay, Z.; Havecker, M.; Knop-Gericke, A.; Jackson, S. D.; Schlögl, R. The Roles of Subsurface Carbon and Hydrogen in Palladium-Catalyzed Alkyne Hydrogenation. *Science* **2008,** *320*, 86–89.

(20) Christmann, K. Some General-Aspects of Hydrogen Chemisorption on Metal-Surfaces. *Prog. Surf. Sci.* **1995,** *48*, 15–26.

(21) Mitsui, T.; Rose, M. K.; Fomin, E.; Ogletree, D. F.; Salmeron, M. Hydrogen Adsorption and Diffusion on Pd(111). *Surf. Sci.* **2003,** *540*, 5–11.

(22) Mitsui, T.; Rose, M. K.; Fomin, E.; Ogletree, D. F.; Salmeron, M. Dissociative Hydrogen Adsorption on Palladium Requires Aggregates of Three or More Vacancies. *Nature* **2003,** *422*, 705–707.

(23) Ferris, J. H.; Kushmerick, J. G.; Johnson, J. A.; Youngquist, M. G. Y.; Kessinger, R. B.; Kingsbury, H. F.; Weiss, P. S. Design, Operation, and Housing of an Ultrastable, Low Temperature, Ultrahigh Vacuum Scanning Tunneling Microscope. *Rev. Sci. Instrum.* **1998,** *69*, 2691–2695.

(24) Conrad, H.; Ertl, G.; Latta, E. E. Adsorption of Hydrogen on Palladium Single-Crystal Surfaces. *Surf. Sci.* **1974,** *41*, 435–446.

(25) Böhringer, M.; Berndt, R.; Schneider, W. D. Transition from Three-Dimensional to Two-Dimensional Faceting of Ag(110) Induced by Cu-Phthalocyanine. *Phys. Rev. B* **1997,** *55*, 1384–1387.

(26) Chaika, A. N.; Nazin, S. S.; Bozhko, S. I. Selective STM Imaging of Oxygen-Induced Cu(115) Surface Reconstructions with Tungsten Probes. *Surf. Sci.* **2008,** *602*, 2078–2088.

(27) Chen, Q.; Richardson, N. V. Surface Facetting Induced by Adsorbates. *Prog. Surf. Sci.* **2003,** *73*, 59–77.

(28) Ozcomert, J. S.; Pai, W. W.; Bartelt, N. C.; Reuttrobey, J. E. Kinetics of Oxygen-Induced Faceting of Vicinal Ag(110). *Phys. Rev. Lett.* **1994,** *72*, 258–261.

(29) Pascual, J. I.; Barth, J. V.; Ceballos, G.; Trimarchi, G.; De Vita, A.; Kern, K.; Rust, H. P. Mesoscopic Chiral Reshaping of the Ag(110) Surface Induced by the Organic Molecule PVBA. *J. Chem. Phys.* **2004,** *120*, 11367–11370.

(30) Lachenwitzer, A.; Morin, S.; Magnussen, O. M.; Behm, R. J. In Situ STM Study of Electrodeposition and Anodic Dissolution of Ni on Ag(111). *Phys. Chem. Chem. Phys.* **2001,** *3*, 3351–3363.

(31) Seehofer, L.; Huhs, S.; Falkenberg, G.; Johnson, R. L. Gold-Induced Faceting of Si(111). *Surf. Sci.* **1995,** *329*, 157–166.

(32) Sutter, P.; Zahl, P.; Sutter, E. Continuous Formation and Faceting of SiGe Islands on Si(100). *Appl. Phys. Lett.* **2003,** *82*, 3454–3456.

(33) Guan, J.; Campbell, R. A.; Madey, T. E. Ultrathin Metal-Films on W(111) - Morphology and Faceting Reconstruction. *Surf. Sci.* **1995,** *341*, 311–327.

(34) Madey, T. E.; Guan, J.; Dong, C. Z.; Shivaprasad, S. M. Morphological Instabilities Induced by Ultrathin Films on W(111). *Surf. Sci.* **1993,** *287*, 826–830.

(35) Madey, T. E.; Guan, J.; Nien, C. H.; Dong, C. Z.; Tao, H. S.; Campbell, R. A. Faceting Induced by Ultrathin Metal Films on W(111) and Mo(111): Structure, Reactivity, and Electronic Properties. *Surf. Rev. Lett.* **1996,** *3*, 1315–1328.

(36) Nien, C. H.; Madey, T. E.; Tai, Y. W.; Leung, T. C.; Che, J. G.; Chan, C. T. Coexistence of {011} Facets with {112} Facets on W(111) Induced by Ultrathin Films of Pd. *Phys. Rev. B* **1999,** *59*, 10335–10340.

(37) Knight, P. J.; Driver, S. M.; Woodruff, D. P. Oxygen-Induced Step-Edge Faceting; A Precursor to (410) Planar Faceting of Cu(100) Vicinal Surfaces. *Chem. Phys. Lett.* **1996,** *259*, 503–507.

(38) Andreasen, G.; Visintin, A.; Salvarezza, R. C.; Triaca, W. E.; Arvia, A. J. Hydrogen-Induced Deformations of Metals Followed by *In Situ* Scanning Tunneling Microscopy, Palladium Electrolytic Hydrogen Charging and Discharging in Alkaline Solution. *Langmuir* **1999,** *15*, 1–5.

(39) Méndez, J.; Gómez-Herrero, J.; Pascual, J. I.; Baró, A. M. Formation of New Terraces Via Diffusion Induced by the Field Gradient in Scanning Tunneling Microscopy. *Appl. Phys. A: Mater. Sci. Process.* **1998,** *66*, S767–S769.

(40) Behm, R. J. Local Structures and Processes on Surfaces Studied by Scanning Tunneling Microscopy. *J. Phys.: Condens. Matter* **1991,** *3*, S117–S120.

(41) Greeley, J.; Mavrikakis, M. Surface and Subsurface Hydrogen: Adsorption Properties on Transition Metals and Near-Surface Alloys. *J. Phys. Chem. B* **2005,** *109*, 3460–3471.

(42) Ichihara, S.; Okuyama, H.; Kato, H.; Kawai, M.; Domen, K. Two Adsorption States of $C_2h_4$ at Saturation Coverage on Pd(110)-(2 × 1)-H. *Chem. Lett.* **2000,** 112–113.

(43) Ledentu, V.; Dong, W.; Sautet, P.; Kresse, G.; Hafner, J. H-Induced Reconstructions on Pd(110). *Phys. Rev. B* **1998,** *57*, 12482–12491.

(44) Memmert, U.; He, J. W.; Griffiths, K.; Lennard, W. N.; Norton, P. R.; Richardson, N. V.; Jackman, T. E.; Unertl, W. N. $D_2$ on Pd(110) - Surface and Subsurface Phases, Absolute Coverages, and Interconversion. *J. Vac. Sci. Technol., A* **1989,** *7*, 2152–2154.

(45) Minca, M.; Penner, S.; Loerting, T.; Menzel, A.; Bertel, E.; Zucca, R.; Redinger, J. Chemisorption of Hydrogen on the Missing-Row Pt(110)-(1 × 2) Surface. *Top. Catal.* **2007,** *46*, 161–167.

(46) Muschiol, U.; Schmidt, P. K.; Christmann, K. Adsorption and Absorption of Hydrogen on a Palladium (210) Surface: A Combined LEED, TDS, $\Delta\Phi$ and HREELS Study. *Surf. Sci.* **1998,** *395*, 182–204.

(47) Skottke, M.; Behm, R. J.; Ertl, G.; Penka, V.; Moritz, W. LEED Structure-Analysis of the Clean and (2 × 1)H Covered Pd(110) Surface. *J. Chem. Phys.* **1987,** *87*, 6191–6198.

(48) Tománek, D.; Sun, Z.; Louie, S. G. Ab Initio Calculation of Chemisorption Systems - H on Pd(001) and Pd(110). *Phys. Rev. B* **1991,** *43*, 4699–4713.

(49) Yoshinobu, J.; Tanaka, H.; Kawai, M. Elucidation of Hydrogen-Induced (1 × 2) Reconstructed Structures on Pd(110) from 100 to 300 K by Scanning-Tunneling-Microscopy. *Phys. Rev. B* **1995,** *51*, 4529–4532.

(50) Kampshoff, E.; Waelchli, N.; Menck, A.; Kern, K. Hydrogen-Induced Missing-Row Reconstructions of Pd(110) Studied by Scanning Tunneling Microscopy. *Surf. Sci.* **1996,** *360*, 55–60.

(51) Niehus, H.; Hiller, C.; Comsa, G. Row Pairing Induced by Hydrogen Adsorption at Pd(110). *Surf. Sci.* **1986,** *173*, L599–L605.

(52) Kralj, M.; Becker, C.; Wandelt, K. The Initial Stages of the Hydrogen-Induced Reconstruction of Pd(110) Studied with STM. *Surf. Sci.* **2006,** *600*, 4113–4118.





DOI: 10.1021/jz100640y | *J. Phys. Chem. Lett.* **2010,** *1*, 2288–2294

(53) Benson, J. W.; Schrader, G. L.; Angelici, R. J. Studies of the Mechanism of Thiophene Hydrodesulfurrization: $^2$H NMR and Mass-Spectral Analysis of 1,3-Butadiene Produced in the Deuterodesulfurization (DDS) of Thiophene over $PbMo_6S_8$ Catalyst. *J. Mol. Catal. A: Chem.* **1995,** *96*, 283–299.
(54) Choi, M. G.; Daniels, L. M.; Angelici, R. J. Synthesis and Desulfurization of 2,5-Dihydrothiophene Transition-Metal Complexes - Models for the Hydrodesulfurization (HDS) of Thiophene. *Inorg. Chem.* **1991,** *30*, 3647–3651.
(55) Diemann, E.; Weber, T.; Müller, A. Modeling the Thiophene HDS Reaction on a Molecular-Level. *J. Catal.* **1994,** *148*, 288–303.
(56) Xu, H.; Friend, C. M. Effect of Sulfur on Desulfurization Kinetics and Selectivity: 2,5-Dihydrothiophene on Mo(110)-(4 ×1)-S. *J. Phys. Chem.* **1993,** *97*, 3584–3590.
(57) Kushmerick, J. G.; Kandel, S. A.; Han, P.; Johnson, J. A.; Weiss, P. S. Atomic-Scale Insights into Hydrodesulfurization. *J. Phys. Chem. B* **2000,** *104*, 2980–2988.
(58) Futaba, D. N.; Chiang, S. Calculations of Scanning Tunneling Microscopic Images of Benzene on Pt(111) and Pd(111), and Thiophene on Pd(111). *Jpn. J. Appl. Phys., Part 1* **1999,** *38*, 3809–3812.
(59) Avouris, P.; Lyo, I. W.; Molinasmata, P. STM Studies of the Interaction of Surface-State Electrons on Metals with Steps and Adsorbates. *Chem. Phys. Lett.* **1995,** *240*, 423–428.
(60) Dahl, S.; Logadottir, A.; Egeberg, R. C.; Larsen, J. H.; Chorkendorff, I.; Törnqvist, E.; Nørskov, J. K. Role of Steps in $N_2$ Activation on Ru(0001). *Phys. Rev. Lett.* **1999,** *83*, 1814–1817.
(61) Gambardella, P.; Šljivančanin, Ž.; Hammer, B.; Blanc, M.; Kuhnke, K.; Kern, K. Oxygen Dissociation at Pt Steps. *Phys. Rev. Lett.* **2001,** *87*, 056103.
(62) Guo, X. C.; Madix, R. J. Site-Specific Reactivity of Oxygen at Cu(110) Step Defects: An STM Study of Ammonia Dehydrogenation. *Surf. Sci.* **1996,** *367*, L95–L101.
(63) Kamna, M. M.; Stranick, S. J.; Weiss, P. S. Imaging Substrate-Mediated Interactions. *Science* **1996,** *274*, 118–119.
(64) Nakano, H.; Nakamura, J. Carbide-Induced Reconstruction Initiated at Step Edges on Ni(111). *Surf. Sci.* **2001,** *482*, 341–345.
(65) Smoluchowski, R. Anisotropy of the Electronic Work Function of Metals. *Phys. Rev.* **1941,** *60*, 661–674.
(66) Stranick, S. J.; Kamna, M. M.; Weiss, P. S. Atomic-Scale Dynamics of a 2-Dimensional Gas-Solid. *Interface Sci.* **1994,** *266*, 99–102.
(67) Sykes, E. C. H.; Han, P.; Weiss, P. S. Molecule/Metal Surface Interactions Evidenced Quantum Mechanically via Tip-Induced $CS_2$ Interaction with Friedel Oscillations on Au{111}. *J. Phys. Chem. B* **2003,** *107*, 5016–5021.
(68) Vang, R. T.; Honkala, K.; Dahl, S.; Vestergaard, E. K.; Schnadt, J.; Lægsgaard, E.; Clausen, B. S.; Nørskov, J. K.; Besenbacher, F. Ethylene Dissociation on Flat and Stepped Ni(111): A Combined STM and DFT Study. *Surf. Sci.* **2006,** *600*, 66–77.
(69) Weiss, P. S.; Eigler, D. M. Adsorption and Accommodation of Xe on Pt{111}. *Phys. Rev. Lett.* **1992,** *69*, 2240–2243.
(70) Yoon, H. A.; Salmeron, M.; Somorjai, G. A. Scanning Tunneling Microscopy (STM) Study of Benzene and Its Coadsorption with Carbon Monoxide on Rh(111). *Surf. Sci.* **1997,** *373*, 300–306.
(71) Zambelli, T.; Wintterlin, J.; Trost, J.; Ertl, G. Identification of the "Active Sites" of a Surface-Catalyzed Reaction. *Science* **1996,** *273*, 1688–1690.
(72) Tierney, H. L.; Baber, A. E.; Sykes, E. C. H. Atomic-Scale Imaging and Electronic Structure Determination of Catalytic Sites on Pd/Cu near Surface Alloys. *J. Phys. Chem. C* **2009,** *113*, 7246–7250.
(73) Blake, M. M.; Nanayakkara, S. U.; Claridge, S. A.; Fernández-Torres, L. C.; Sykes, E. C. H.; Weiss, P. S. Identifying Reactive Intermediates in the Ullmann Coupling Reaction by Scanning Tunneling Microscopy and Spectroscopy. *J. Phys. Chem. A* **2009,** *113*, 13167–13172.
(74) Somorjai, G. A. The Flexible Surface - Correlation between Reactivity and Restructuring Ability. *Langmuir* **1991,** *7*, 3176–3182.
(75) Somorjai, G. A. The Flexible Surface: New Techniques for Molecular Level Studies of Time Dependent Changes in Metal Surface Structure and Adsorbate Structure during Catalytic Reactions. *J. Mol. Catal. A: Chem.* **1996,** *107*, 39–53.
(76) Meyer, J. A.; Stranick, S. J.; Wang, J. B.; Weiss, P. S. Field-Emission Current Voltage Curves as a Diagnostic for Scanning Tunneling Microscope Tips. *Ultramicroscopy* **1992,** *42*, 1538–1541.



DOI: 10.1021/jz100640y | *J. Phys. Chem. Lett.* **2010,** *1*, 2288–2294